J|A|C|S COMMUNICATIONS

Published on Web 08/24/2010

Self-Propagating Molecular Assemblies as Interlayers for Efficient Inverted Bulk-Heterojunction Solar Cells

Leila Motiei,[†] Yan Yao,[‡] Joyanta Choudhury,[†] He Yan,[‡] Tobin J. Marks,*[,§] Milko E. van der Boom,*[,†] and Antonio Facchetti*[,‡,§]

Department of Organic Chemistry, The Weizmann Institute of Science, Rehovot 76100, Israel, Polyera Corporation, 8045 Lamon Avenue, Skokie, Illinois 60077, Department of Chemistry and the Argonne-Northwestern Solar Energy Research Center, and the Materials Research Center, Northwestern University, Evanston, Illinois 60208

Received May 30, 2010; E-mail: milko.vanderboom@weizmann.ac.il; t-marks@northwestern.edu; afacchetti@polyera.com

Abstract: Here we report the first use of self-propagating molecule-based assemblies (SPMAs) as efficient electron-transporting layers for inverted organic photovoltaic (OPV) cells. P3HT-PCBM cells functionalized with optimized SPMAs exhibit power conversion efficiencies approaching 3.6% (open circuit voltage = 0.6 V) vs 1.5% and 2.4% for the bare ITO and Cs_2CO_3-coated devices, respectively. The dependence of cell response parameters on interlayer thickness is investigated, providing insight into how to further optimize device performance.

Bulk-heterojunction organic photovoltaic (BHJ OPV) cells have attracted considerable attention as testbeds to: (i) probe fundamental charge transfer/transport processes in organic solids, (ii) develop unconventional electronic materials and processing, and (iii) enable low-cost, mechanically flexible PV technologies as complementary to inorganic semiconductors.[1] In the past two years, the discovery of novel molecular and polymeric photoactive donors and interfacial layers has enabled the development of OPV cells with large power conversion efficiencies (PCEs).[2] Most of these efficient cells are based on a conventional architecture consisting of substrate (glass, plastic)/indium−tin oxide (ITO)/PEDOT:PSS/photoactive donor−acceptor blend/Ca (or LiF)/Al. Device performance often degrades because of morphological changes in the photoactive layer, instability of the ITO/PEDOT:PSS interface,[2d] and oxidation of the cathode.[3a] Furthermore, low workfunction metals are difficult to print. Thus, OPV cells based on the aforementioned design are far from ideal, making the transition to large-area modules challenging.[3b]

To address these challenges, inverted geometry OPV cells consisting of ITO-coated substrates and a top metal contact have been developed.[4] Here the electrode functions are reversed, with holes and electrons now extracted by the metal and ITO, respectively. Typical inverted architectures consist of substrate-ITO/electron transport layer/photoactive blend/hole transport layer/Ag (or Au).[4] The stability of these inverted solar cells can be enhanced by deleting the ITO/PEDOT:PSS interface and using an air-stable metal anode.[4c,f] In addition, inverted OPVs may exhibit larger external quantum efficiencies (EQEs) because PEDOT:PSS absorption losses can be minimized with an appropriate electron-transporting layer.[4e,i] Finally, it has been shown that the vertical phase separation of several photoactive blends results in a more favorable morphology in inverted OPV architectures.[5]

Key to inverted OPV cell performance is the electron-transporting material that functions as an electron-transport/hole-blocking layer. Critical requirements to simultaneously satisfy for an effective interlayer are as follows: (i) *Energetics:* the interlayer HOMO must lie lower than the donor material HOMO, whereas the interlayer LUMO energy should be similar to that of the electron acceptor. (ii) *Solubility orthogonality*: The interlayer should be insoluble in solvents used for active layer deposition. (iii) *Film morphology*: the interlayer should be smooth and contiguous. (iv) *Conductivity*: the interlayer should be sufficiently conductive to minimize parasitic resistance and not be overly photosensitive.[5b]

Amorphous transition metal oxides such as TiO_x[4a−d] and ZnO[4e,f] have been used as interlayers in inverted cells due to their large band gaps and conduction bands well-aligned with fullerene LUMOs, the most commonly used electron acceptor materials. However, if sol−gel chemistry is used for the metal oxide film, it is difficult to control film morphology, chemical composition, and conductivity, particularly at low processing temperatures. An alternative approach employs alkali metal salts such as Cs_2CO_3 which alters the ITO work function[4g−i] by forming an interfacial dipole layer.[4h] However, to the best of our knowledge, tailorable metal−organic interlayers have not been employed in inverted OPV cell fabrication. Here we report the use of two self-propagating molecule-based assemblies (SPMAs)[6] as efficient electron-transporting layers for inverted OPVs.

SPMAs of various thicknesses were fabricated by iterative immersion of $ClCH_2$-Ph-Si-coated ITO/glass substrates in solutions of **1** or **2** and $(PhCN)_2PdCl_2$ (Figure 1A),[6] where the benzonitrile ligands are readily replaced by substituted pyridines. SPMA thickness was measured by ellipsometry on Si substrates and can be controlled by the number of alternating complex-$PdCl_2$ layers. SPMA-**1** and SPMA-**2** optical spectra exhibit a similar λ_{max} at ∼490 nm. (Figure S1). Cyclic voltammetry of the SPMAs on ITO reveals reversible $Ru^{2+/3+}$ redox chemistry (Figure S2).

A mixture of poly(3-hexylthiophene):[6,6]-phenyl C61 butyric acid methyl ester (P3HT:PCBM) was used here as the photoactive blend for OPV fabrication and to demonstrate interlayer function. Figures 1B and 1C show details of the device structure and the energy levels of the component materials. The LUMO and HOMO energies of the **1**- and **2**-based SPMAs are ∼ −4.0 and −6.0 eV, respectively. Owing to the comparable SPMA and PCBM LUMO energies, and the SPMA and P3HT HOMO energy barriers, the interface should transport electrons and block holes on the ITO side. V_2O_5 was used as a hole-transporting/electron-blocking layer on the Al side,[4g] thus inverting the device polarity. BHJ OPVs were fabricated by spin-coating a solution of P3HT + PCBM in chlorobenzene (10:8 mg/mL, 700 rpm for 50 s) onto ITO/SPMA as well as bare ITO and Cs_2CO_3/ITO control devices. The active layer thickness is 80−90 nm. Next, the substrates were annealed on a hot plate at 150 °C for 10 min under nitrogen. Subsequently,

[†] The Weizmann Institute of Science.
[‡] Polyera Corporation.
[§] Northwestern University.

10.1021/ja104695p

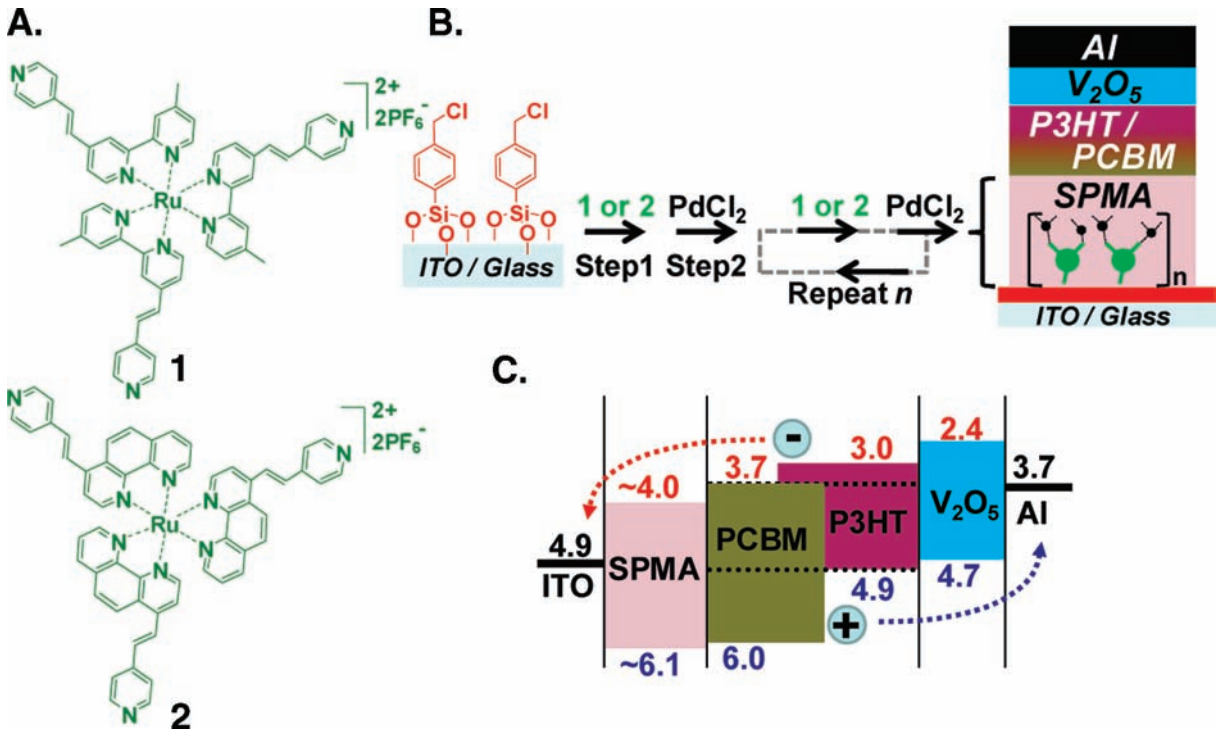

Figure 1. (A) Ruthenium complexes used for SPMA fabrication on ITO/glass substrates via pyridyl-$PdCl_2$ coordination.[6] (B) Inverted solar cell structure. (C) Approximate energy level diagram (in eV) for the materials used in cell fabrication.

10 nm V_2O_5 and 80 nm Al layers were vacuum-evaporated to complete the devices. Note that although quantification of V_2O_5 and other metal oxide thin film energy levels are still under debate,[7a,b] several groups have successfully used V_2O_5 for inverted OPV fabrication.[7c,d,5]

Figures 2 and S3 show representative $J-V$ measurements under illumination and in the dark, and Figure S4 represents an EQE plot for SPMA-**2**. OPV performance parameters are summarized in Tables 1 and S1. The dark $J-V$ curves for the inverted solar cell, based on a bare ITO substrate, exhibit low current in the forward direction and a high leakage current in the reverse direction. As expected, ITO alone cannot extract electrons and block holes, and the bare-ITO-based OPVs perform poorly (V_{oc} = 0.38 V, PCE ~1.5%). Using the SPMAs as interfacial layers, the electron selectivity of the bottom contact improves significantly. The shunt resistance increases greatly from 4.0×10^3 $\Omega \cdot cm^2$ to 1.1×10^6 $\Omega \cdot cm^2$, and the series resistance falls from 3.0 $\Omega \cdot cm^2$ to 2.7 $\Omega \cdot cm^2$. The improved carrier selectivity is also reflected by the increased open circuit voltage (V_{oc} = 0.6 V) and fill factor (FF; 43.8% → 57.3%), resulting in PCEs approaching 3.6%. The performance of Cs_2CO_3/ITO lies in between that of the bare and SPMA-functionalized devices, with PCE = 2.4%. Compared to the bare ITO devices, J_{sc} increases to 10.1 mA/cm^2, V_{oc} increases to 0.48 V, and FF increases to 49.0%. However, the shunt resistance is only 1.7×10^4 $\Omega \cdot cm^2$, which is 10−100× lower than that of SPMA-based devices. Note that with Cs_2CO_3 as an interlayer, the maximum reported PCE (~4%) was achieved using P3HT-PCBM.[4i] This performance results from the far greater photoactive layer thickness of 210−230 nm vs the 80−90 nm used here. Since spun-cast Cs_2CO_3 films cover the ITO[4h] surface unevenly, thick photoactive films must be used to suppress leakage currents/increase shunt resistance. In contrast, the relative smooth surface morphology of the ITO-coated SPMA (Figure S5) enables the use of far less photoactive materials.

OPV cell performance was further characterized by varying the number of SPMA deposition steps. Figures 3 and S6 show the dependence of cell parameters on SPMA interlayer type and the number of deposition steps. Note that these SPMAs exhibit nonlinear film growth.[6] Thus, the SPMA-based device efficiency first increases, going from 0 to 3 (for **1**) and 5 (for **2**) complex-

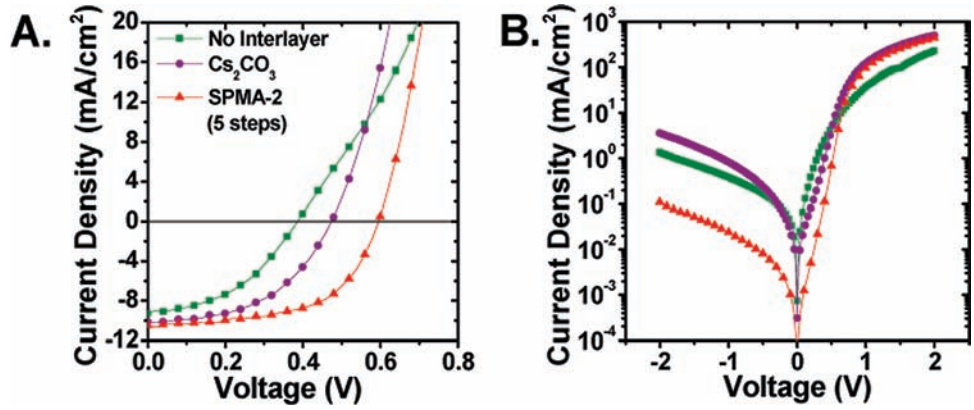

Figure 2. (A) Representative $J-V$ response data for an SPMA-**2** based cell and control cells. (B) Corresponding dark currents.

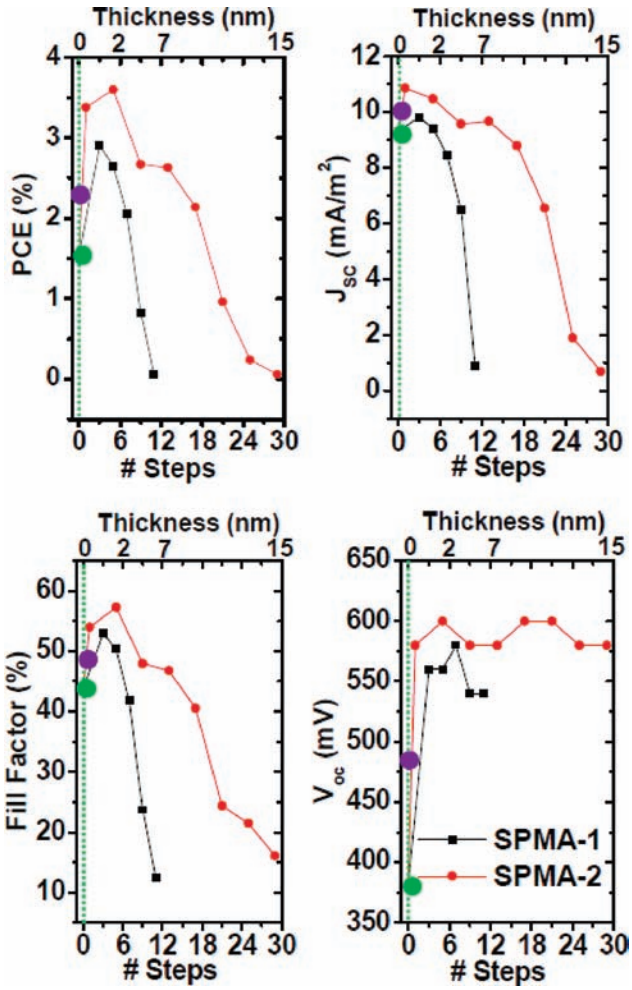

Figure 3. Cell response parameters as a function of the interlayer identity and the number of interlayer deposition steps. The green and purple dots indicate parameter values for the bare ITO and Cs_2CO_3/ITO electrodes, respectively.

$PdCl_2$ layers, and then steadily declines. Both J_{sc} and FF decrease with increasing numbers of SPMA layers, which might reflect limited conductivity of the thick SPMA films. V_{oc} increases and then saturates at ~0.6 V, similar to the typical value for conventional geometry P3HT:PCBM cells. Interestingly, for both interlayer types, devices reach peak efficiency at a film thickness of ~1−2 nm. However, whereas SPMA-**1** cells are inactive at a film thickness of ~5 nm, SPMA-**2** cells exhibit reasonable performance up to a film thickness of ~7−10 nm, probably reflecting the more π-extended phenanthrolyl of **2** vs the bipyridyl ligand of **1**, which enhances the charge transport efficiency of the corresponding **2**-based chelates and SPMA films.[8]

Table 1. Comparison of Solution-Processed Inverted P3HT:PCBM BHJ Photovoltaic Cells Fabricated with the Indicated Interlayers[a,b]

Interlayer	J_{sc} [mA/cm^2]	V_{oc} [V]	FF [%]	PCE [%]	R_{series}[c] [Ω · cm^2]	R_{shunt}[d] [Ω · cm^2]
Bare ITO	9.3	0.38	43.8	1.54	3.0	4×10^3
Cs_2CO_3[e]	10.1	0.48	49.0	2.38	2.5	0.2×10^5
SPMA-**1** (3 steps)	9.8	0.56	52.9	2.91	2.4	0.9×10^5
SPMA-**2** (5 steps)	10.5	0.60	57.3	3.60	2.7	11.0×10^5

[a] General device structure: ITO/interlayer/P3HT:PCBM blend/V_2O_5/Al with ~9 mm^2 device area. [b] All devices characterized under the standard AM1.5G 1 Sun test conditions using instrumentation and published procedures.[2d] PCEs derived from $\eta_p = (J_{sc}V_{oc}FF)/P_o$, where J_{sc} = the short circuit current [mA/cm^2], V_{oc} the open circuit voltage [V], FF the fill factor, and P_o the incident light intensity [mW/cm^2]. [c] Series resistance calculated at 2 V of dark current. [d] Shunt resistance calculated at 0.0 V of dark current. [e] Following procedure reported in ref 4i.

In conclusion, we report the first study of metal−organic multilayers for the fabrication of inverted OPVs. Our results show that device performance is strongly dependent on the interlayer type and thickness. We are currently exploring SPMAs with greater conductivities and based on lower-lying HOMO units to enhance hole-blocking capabilities.

Acknowledgment. This research was supported by a grant from M. K. Schnur, by the US-Israel Binational Science Foundation (BSF), and by the U.S. DOE-BES Argonne-Northwestern Solar Energy Research Center (ANSER), an Energy Frontier Research Center (Award DE-SC0001059). J.C. thanks the EU FP7 program for a Marie Curie fellowship.

Supporting Information Available: Experimental details. This material is available free of charge via the Internet at http://pubs.acs.org.

References

(1) (a) Brabec, C. J.; Scherf. U.; Dyakonov, V. In *Organic Photovoltaics: Materials, Device Physics, and Manufacturing Technologies*; John Wiley & Sons: 2008. (b) Beverina, L.; Salice, P. *Eur. J. Org. Chem.* **2010**, 1207. (c) Gaudiana, R. *J. Phys. Chem. Lett.* **2010**, *1*, 1288. (d) Bredas, J.-L.; Durrant, J. R. *Acc. Chem. Res.* **2009**, *42*, 1689.

(2) (a) Park, S. H.; Roy, A.; Beaupré, S.; Cho, S.; Coates, N.; Moon, J. S.; Moses, D.; Leclerc, M.; Lee, K.; Heeger, A. J. *Nature Photon.* **2009**, *3*, 297. (b) Liang, Y.; Feng, D.; Wu, Y.; Tsai, S. T.; Li, G.; Ray, C.; Yu, L. *J. Am. Chem. Soc.* **2009**, *131*, 7792. (c) Chen, H. Y.; Hou, J.; Zhang, S.; Liang, Y.; Yang, G.; Yang, Y.; Yu, L.; Wu, Y.; Li, G. *Nature Photon.* **2009**, *3*, 649. (d) Silvestri, F.; Lopez-Duarte, I.; Seitz, W.; Beverina, L.; Martinez-Diaz, M. V.; Marks, T. J.; Guldi, D. M.; Pagani, G. A.; Torres, T. *Chem. Commun.* **2009**, 4500. (e) Irwin, M. D.; Buchholz, D. B.; Hains, A. W.; Chang, R. P. H.; Marks, T. J. *Proc. Natl. Acad. Sci. U.S.A.* **2008**, *105*, 2783.

(3) (a) de Jong, M. P.; van IJzendoorn, L. J.; de Voigt, M. J. A. *Appl. Phys. Lett.* **2000**, *77*, 2255. (b) Krebs, F. C.; Gevorgyan, S. A.; Alstrup, J. *J. Mater. Chem.* **2009**, *19*, 5442.

(4) (a) Waldauf, C.; Morana, M.; Denk, P.; Schilinsky, P.; Coakley, K.; Choulis, S. A.; Brabec, C. J. *Appl. Phys. Lett.* **2006**, *89*, 233517. (b) Steim, R.; Choulis, S. A.; Schilinsky, P.; Brabec, C. J. *Appl. Phys. Lett.* **2008**, *92*, 093303. (c) Kim, C. S.; Lee, S. S.; Gomez, E. D.; Kim, J. B.; Loo, Y. L. *Appl. Phys. Lett.* **2009**, *94*, 113302. (d) Kim, C. S.; Tinker, L. L.; DiSalle, B. F.; Gomez, E. D.; Lee, S.; Bernhard, S.; Loo, Y. L. *Adv. Mater.* **2009**, *21*, 3110. (e) White, M. S.; Olson, D. C.; Shaheen, S. E.; Kopidakis, N.; Ginley, D. S. *Appl. Phys. Lett.* **2006**, *89*, 143517. (f) Hau, S. K.; Yip, H. L.; Baek, N. S.; Zou, J.; O'Malley, K.; Jen, A. K. Y. *Appl. Phys. Lett.* **2008**, *92*, 253301. (g) Li, G.; Chu, C. W.; Shrotriya, V.; Huang, J.; Yang, Y. *Appl. Phys. Lett.* **2006**, *88*, 253503. (h) Huang, J.; Li, G.; Yang, Y. *Adv. Mater.* **2008**, *20*, 415. (i) Liao, H. H.; Chen, L. M.; Xu, Z.; Li, G.; Yang, Y. *Appl. Phys. Lett.* **2008**, *92*, 173303. (j) Kim, C. S.; Lee, S.; Tinker, L. L.; Bernhard, S.; Loo, Y.-L. *Chem. Mater.* **2009**, *21*, 4583.

(5) (a) Yao, Y.; Hou, J.; Xu, Z.; Li, G.; Yang, Y. *Adv. Funct. Mater.* **2008**, *18*, 1783. (b) Xu, Z.; Chen, L. M.; Yang, G.; Huang, C. H.; Hou, J.; Wu, Y.; Li, G.; Hsu, C. S.; Yang, Y. *Adv. Funct. Mater.* **2009**, *19*, 1227.

(6) (a) Motiei, L.; Lahav, M.; Gulino, A.; Iron, M. A.; van der Boom, M. E. *J. Phys. Chem. B* **2010**, ASAP, DOI: 10.1021/jp910898f. (b) Choudhury, J.; Kaminker, R.; Motiei, L.; de Ruiter, G.; Morozov, M.; Lupo, F.; Gulino, A.; van der Boom, M. E. *J. Am. Chem. Soc.* **2010**, *132*, 9295. (c) Motiei, L.; Altman, M.; Gupta, T.; Lupo, F.; Gulino, A.; Evmenenko, G.; Dutta, P.; van der Boom, M. E. *J. Am. Chem. Soc.* **2008**, *130*, 8913. (d) See Supporting Information.

(7) (a) Ding, I. H.; Gao, Y.; Kim, D. Y.; Subbiah, J.; So, F. *Appl. Phys. Lett.* **2010**, *96*, 073304. (b) Hamwi, S.; Meyer, J.; Kröger, M.; Winkler, T.; Witte, M.; Riedl, T.; Kahn, A.; Kowalsky, W. *Adv. Funct. Mater.* **2010**, *20*, 1762. (c) Zhu, X. L.; Sun, J. X.; Peng, H. J.; Meng, Z. G.; Wong, M.; Kwok, H. S. *Appl. Phys. Lett.* **2005**, *87*, 153508. (d) Huang, J.-S.; Chou, C.-Y.; Liu, M.-Y.; Tsai, K.-H.; Lin, W.-H.; Lin, C.-F. *Org. Electron.* **2009**, *10*, 1060.

(8) Hurrell, H. C.; Abruna, H. D. *Inorg. Chem.* **1990**, *29*, 736.

JA104695P